

RESEARCH ARTICLE

Nrf2 deficiency causes hepatocyte dedifferentiation and reduced albumin production in an experimental extrahepatic cholestasis model

Guo-Ying Wang^{1,2,3}, Veronica Garcia¹, Joonyong Lee¹, Jennifer Yanum¹, Jingmei Lin⁴, Huaizhou Jiang^{1,5*}, Guoli Dai^{1*}

1 Department of Biology, Center for Developmental and Regenerative Biology, School of Science, Indiana University-Purdue University Indianapolis, Indianapolis, IN, United States of America, **2** Department of Hepatobiliary Surgery, The First Affiliated Hospital of Guangzhou Medical University, Guangzhou, China, **3** Department of Hepatic Surgery and Liver Transplantation Center, The Third Affiliated Hospital, Sun Yet-Sen University, Guangdong, China, **4** Department of Pathology and Laboratory Medicine, Indiana University School of Medicine, Indianapolis, IN, United States of America, **5** School of Traditional Chinese Medicine, Anhui University of Chinese Medicine, Anhui, China

* huazhou@iu.edu (HJ); gdai@iupui.edu (GD)



OPEN ACCESS

Citation: Wang G-Y, Garcia V, Lee J, Yanum J, Lin J, Jiang H, et al. (2022) Nrf2 deficiency causes hepatocyte dedifferentiation and reduced albumin production in an experimental extrahepatic cholestasis model. *PLoS ONE* 17(6): e0269383. <https://doi.org/10.1371/journal.pone.0269383>

Editor: Gianfranco D. Alpini, Texas A&M University, UNITED STATES

Received: February 7, 2022

Accepted: May 19, 2022

Published: June 13, 2022

Copyright: © 2022 Wang et al. This is an open access article distributed under the terms of the [Creative Commons Attribution License](https://creativecommons.org/licenses/by/4.0/), which permits unrestricted use, distribution, and reproduction in any medium, provided the original author and source are credited.

Data Availability Statement: All relevant data are within the paper and its [Supporting Information](#) files.

Funding: The research was supported by a grant from the National Institutes of Health (grant number 1R01DK117076).

Competing interests: The authors have declared that no competing interests exist.

Abstract

The transcription factor Nrf2 modulates the initiation and progression of a number of diseases including liver disorders. We evaluated whether Nrf2 mediates hepatic adaptive responses to cholestasis. Wild-type and Nrf2-null mice were subjected to bile duct ligation (BDL) or a sham operation. As cholestasis progressed to day 15 post-BDL, hepatocytes in the wild-type mice exhibited a tendency to dedifferentiate, indicated by the very weak expression of hepatic progenitor markers: CD133 and tumor necrosis factor-like weak induced apoptosis receptor (Fn14). During the same period, Nrf2 deficiency augmented this tendency, manifested by higher CD133 expression, earlier, stronger, and continuous induction of Fn14 expression, and markedly reduced albumin production. Remarkably, as cholestasis advanced to the late stage (40 days after BDL), hepatocytes in the wild-type mice exhibited a Fn14+ phenotype and strikingly upregulated the expression of deleted in malignant brain tumor 1 (DMBT1), a protein essential for epithelial differentiation during development. In contrast, at this stage, hepatocytes in the Nrf2-null mice entirely inhibited the upregulation of DMBT1 expression, displayed a strong CD133+/Fn14+ phenotype indicative of severe dedifferentiation, and persistently reduced albumin production. We revealed that Nrf2 maintains hepatocytes in the differentiated state potentially via the increased activity of the Nrf2/DMBT1 pathway during cholestasis.

Introduction

Nuclear factor erythroid 2-related factor 2 (Nrf2) is a leucine zipper motif-containing transcription factor [1]. It primarily functions as a redox sensor and maintains redox homeostasis in a

variety of organ systems. Upon activation, it exerts many beneficial effects, such as anti-oxidation, detoxification, anti-inflammation, and anti-apoptosis. During the past several decades, significant insights have been gained regarding its epigenetic and non-epigenetic regulation, activation mechanisms, target genes, and roles in health and disease [2–5]. Nrf2 participates in modulating the initiation and progression of many pathological processes, including liver disorders, and has proven to be a promising target for the prevention and treatment of several diseases [6].

Obstructive extrahepatic cholestasis in humans is widely modeled in rodents by common bile duct ligation (BDL). BDL induces accumulation of the bile constituents, including bile acids, cholesterol, and bilirubin in the liver and blood, thereby causing oxidative stress and secondary liver injury [7–9]. Nrf2 regulates the expression of genes that are critical not only for cellular defense against oxidative stress but also for bile acid synthesis and the enterohepatic circulation of bile acids, playing essential roles in maintaining bile acid homeostasis [10]. During cholestasis, the liver exhibits adaptive responses, including Nrf2 activation, to alleviate liver injury [10–12]. Genetic overactivation of Nrf2 via knockdown of its inhibitor Kelch-like ECH-associated protein 1 (Keap1) or pharmacological activation of Nrf2 counteracts the effects of cholestatic liver injury [12, 13]. However, several studies have demonstrated that the lack of Nrf2 does not cause worsened liver injury in BDL-induced extrahepatic cholestasis or alpha-naphthylisothiocyanate-induced intrahepatic cholestasis [10–12]. These observations have contributed to Nrf2 absence-induced reductions in bile acid synthesis, excretion, and reabsorption, as well as an increase in bile acid hydroxylation and other unknown Nrf2-dependent mechanisms. Here, we aimed to gain further insights into how Nrf2 modulates hepatic adaptive responses to cholestasis.

Materials and methods

Mice and surgical procedures

Nrf2^{+/+} and Nrf2^{-/-} male mice (6-month-old) with a C57BL6/129SV mixed background were used [1]. The mice were housed in plastic cages at 22 ± 1 °C on a 12 h light/dark cycle with lights on from 6:00 am to 6:00 pm. Standard rodent chow and water were provided *ad libitum* throughout the acclimatization period. The BDL and sham operation surgical procedures were performed under aseptic conditions. Mice were anesthetized using an isoflurane inhalation agent. The common bile duct was ligated with two ligatures separated by 2 mm. A cut was made between the two ligatures. Control mice underwent a sham operation that consisted of exposure but no ligation of the common bile duct. Mice were euthanized at 5, 10, 15, 25, and 40 days after the surgeries by decapitation to collect their livers. The livers were immediately excised and weighed. A portion of each liver was fixed in 10% formalin and embedded in paraffin to prepare the liver sections. Meanwhile, part of each liver was frozen in liquid nitrogen to prepare the liver lysates. The remainder of each liver was frozen in liquid nitrogen and stored at -80 °C until further use. All animal experiments were conducted in accordance with the National Institutes of Health (NIH) Guide for the Care and Use of Laboratory Animals and ARRIVE guidelines. Protocols for the care and use of animals were approved by the Indiana University-Purdue University Indianapolis Animal Care and Use Committee.

Histology and immunohistochemistry

Formalin-fixed and paraffin-embedded liver sections were subjected to hematoxylin and eosin (H&E) staining. For each liver section, two 5X magnification non-overlapping images were taken. The area of each necrotic foci on these two images was measured using Image-Pro Plus software (Media Cybernetics, Rockville, MD, USA). The individual areas were added together and then divided by the total area of the two 5X images to generate the total percentage of

necrotic area. Formalin-fixed and paraffin-embedded liver sections were subjected to immunostaining. Primary antibodies against Ki-67 (BS1454; Bioworld, Irving, TX, USA), laminin (L-9393; Sigma-Aldrich, St. Louis, MO, USA), CD133 (14-1331; eBioscience, San Diego, CA, USA), CK19 (SC-33111; Santa Cruz Biotechnology, Dallas, TX, USA); NAD(P)H quinone dehydrogenase 1 (NQO1; A19586; ABclonal, Woburn, MA, USA), Fn14 (ab109365; Abcam, Cambridge, UK), and DMBT1 (AF5195; R&D Systems, Minneapolis MN, USA) were used. Ki67-positive hepatocytes were counted in five randomly chosen microscope fields per section at 200x magnification. Sirius Red-stained areas or CK19 immunostaining-positive areas were quantified using Image-Pro Plus software (Media Cybernetics, Rockville, MD, USA).

Blood biochemistry

Serum alanine aminotransferase (ALT), aspartate aminotransferase (AST), and alkaline phosphatase (ALP) levels were measured with a Hitachi Modular Analyzer (Roche Diagnostics, Indianapolis, IN).

Quantitative real-time polymerase chain reaction (qRT-PCR)

Total RNA was isolated from frozen liver tissue using TRIzol reagent according to the manufacturer's protocol (Invitrogen, Carlsbad, CA, USA). cDNAs were synthesized from the total RNA (1 µg) of each sample using a Verso cDNA Kit (Thermo Scientific, Rockford), diluted four times with water, and subjected to qRT-PCR to quantify mRNA levels. TaqMan Universal PCR Master Mix and the primers and TaqMan MGB probes of mouse *Nrf2* (Mm00477786_m1) and *Nqo1* (Mm01253561_m1) were purchased from Applied Biosystems (Foster City, CA). The amplification reactions were carried out with the ABI Prism 7900 sequence detection system (Applied Biosystems, Foster City, CA) with initial hold steps (50°C for 2 min followed by 95°C for 10 min) and 40 cycles of a 2-step PCR (92°C for 15 seconds and 60°C for 1 min). The comparative CT method was used for the relative quantification of the amount of mRNA in each sample normalized to the *Gapdh* transcript levels.

Western blot analysis

Liver homogenates (10 µg) were separated using polyacrylamide gel electrophoresis under reducing conditions. Proteins from the gels were electrophoretically transferred to polyvinylidene difluoride membranes. Antibodies against NQO1 (2618-1; Epitomics, Burlingame, CA, USA), CD133 (PAB12663; Abnova, Taipei, Taiwan), Fn14 (ab109365; Abcam), DMBT1 (AF5195; R&D Systems), phosphorylated yes-associated protein 1 (p-YAP; S127; 4911; Cell Signaling Technology, Danvers, MA, USA), albumin (A0353, Abclonal, Woburn, MA), YAP (14074; Cell Signaling Technology), p-mammalian target of rapamycin (p-mTOR; S2448; 4911; Cell Signaling Technology), mTOR (2983; Cell Signaling Technology), p-epidermal growth factor receptor (p-EGFR; Y1086; 1139-1; Epitomics), EGFR (1114; Epitomics), and β -catenin (9587; Cell Signaling Technology) were used as probes. Immune complexes were detected using an enhanced chemiluminescence system (Pierce, Rockford, IL, USA). Signals were detected using ImageQuant LAS 4000 Mini (General Electric Life Science, Marlborough, MA) and quantified using ImageJ software.

Statistical analysis

Data are shown as means \pm SD or SEM. Statistical analysis was performed using one-way analysis of variance (ANOVA) or unpaired Student's t-test. Significant differences were defined when $P < 0.05$.

Results

Nrf2 deficiency does not cause broadly worsened liver injury after BDL

We subjected wild-type and Nrf2-null mice to a sham operation or BDL and subsequently performed various assessments at different time points after the surgeries. We found that both genotype groups of mice exhibited markedly increased liver-to-body weight ratios at days 15 and 25 following BDL relative to their sham controls, respectively (Fig 1). The data indicated that, regardless of Nrf2, the livers displayed dramatic enlargement, which was a robust response to BDL during this period (2–4 weeks post-BDL).

During the 40 day period after BDL, the two genotype groups of mice displayed equivalent mortality rates (13.8% in wild-type group vs 10.7% in Nrf2-null group).

BDL-induced liver necrosis was most evident at day 5 after BDL independent of Nrf2 (Fig 2A and 2B). BDL increased serum ALT and AST levels in equivalent magnitudes in both genotype groups of mice at days 5 and 10 after surgery. Relative to Nrf2-null mice, wild-type mice showed lower levels of ALT, but higher AST, at day 15 post-BDL (Fig 2C and 2D). As liver fibrosis advanced, serum concentrations of ALP progressively elevated without a Nrf2-dependent difference (Fig 2E). These data indicate that the lack of Nrf2 may not affect BDL-induced liver injury.

Immunostaining for CK19, a marker of cholangiocytes, revealed similar biliary ductal responses to BDL between the two genotype groups of mice (Fig 3). These findings suggested that Nrf2 might not play a crucial role in the adaptive response of the biliary ducts to cholestasis. Quantification of Ki-67⁺ hepatocytes showed that, irrespective of Nrf2, the hepatocytes underwent massive proliferation at day 5 after BDL, but this event was dramatically weakened thereafter (Fig 4A and 4B), whereas a few replicating hepatocytes were seen in the sham controls. These observations suggested that the presence or absence of Nrf2 might not affect the BDL-induced hepatocyte replication, the first line of repair response to liver injury. Laminin immunostaining showed hepatic septa formation, which was more evident after day 10 post-BDL, without an obvious Nrf2-dependent difference (Fig 5A). Sirius Red staining reflected the

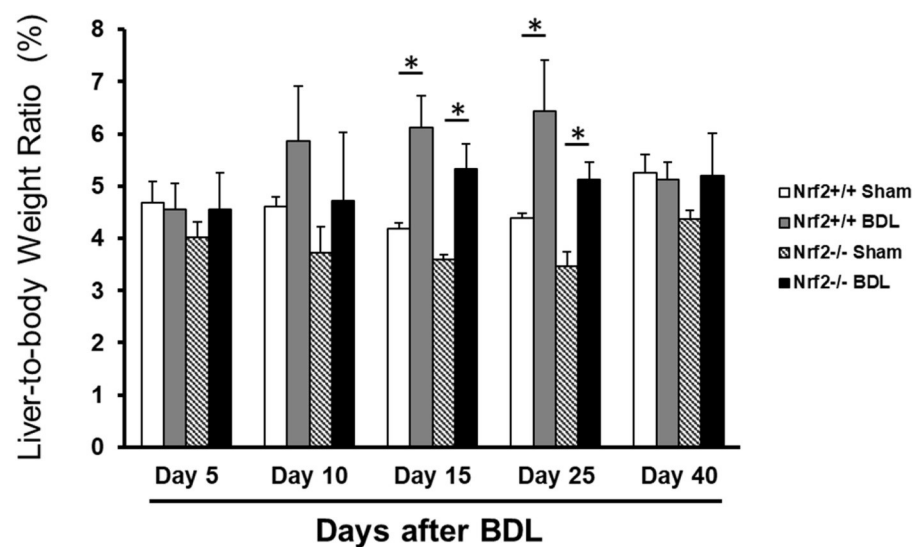


Fig 1. Liver-to-body weight ratios in Nrf2^{+/+} and Nrf2^{-/-} mice after bile duct ligation (BDL) or sham operation (Sham). Adult male mice of both genotypes were subjected to BDL or Sham operation. Mice were sacrificed at the time points indicated. Data are presented as mean liver-to-body weight ratio \pm SD (n = 5). * $P < 0.05$.

<https://doi.org/10.1371/journal.pone.0269383.g001>

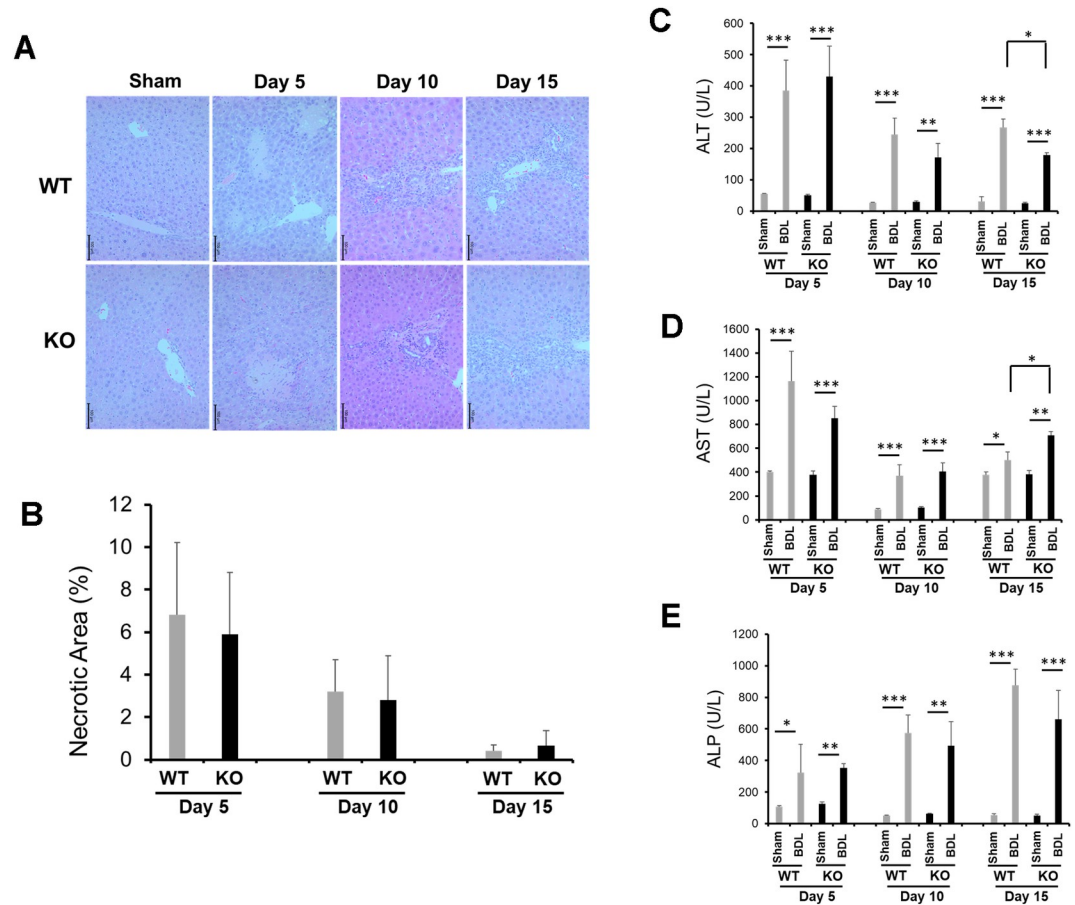


Fig 2. Liver injury in *Nrf2*^{+/+} (WT) and *Nrf2*^{-/-} (KO) mice following bile duct ligation (BDL) or sham operation (Sham). Adult male mice of both genotypes underwent BDL or Sham. (A) Representative images of liver sections stained with H&E. (B) Percentage of necrosis area. Serum concentrations of (C) ALT, (D) AST, and (E) ALP were measured. Data are presented as mean ± SEM (n = 5). **P* < 0.05; ***P* < 0.01; ****P* < 0.001.

<https://doi.org/10.1371/journal.pone.0269383.g002>

hepatic content of collagen (Fig 5B), which was equivalent between the BDL wild-type and *Nrf2*-null mice over the 40 day period (Fig 5C). Taken together, these findings demonstrated that the lack of *Nrf2* does not remarkably affect BDL-induced liver size alteration, biliary ductular reaction, liver repair, and hepatic fibrotic response.

***Nrf2* deficiency causes hepatocyte dedifferentiation in response to BDL**

We next evaluated the functional state of hepatic *Nrf2* by measuring the hepatic expression of *Nrf2* mRNA and *Nqo1* mRNA and protein. *Nqo1* is a typical *Nrf2* target gene that has been shown to be solely regulated by *Nrf2* in BDL-induced cholestasis [11]. We found that, compared to sham controls, BDL did not significantly affect *Nrf2* transcript levels, but elevated *Nqo1* mRNA expression (Fig 6A). NQO1 expression was increased as the cholestasis progressed in wild-type mice, which was fully prevented by the absence of *Nrf2* (Figs 6B and S1). These findings indicate that hepatic *Nrf2* exhibits persistent activation post-transcriptionally in response to BDL, consistent with the result of another study [11].

We next evaluated whether BDL induces a phenotypic response of hepatocytes in an *Nrf2*-dependent manner by screening a subset of molecules associated with hepatocyte differentiation. As a result, we revealed striking *Nrf2*-dependent changes in the expression of

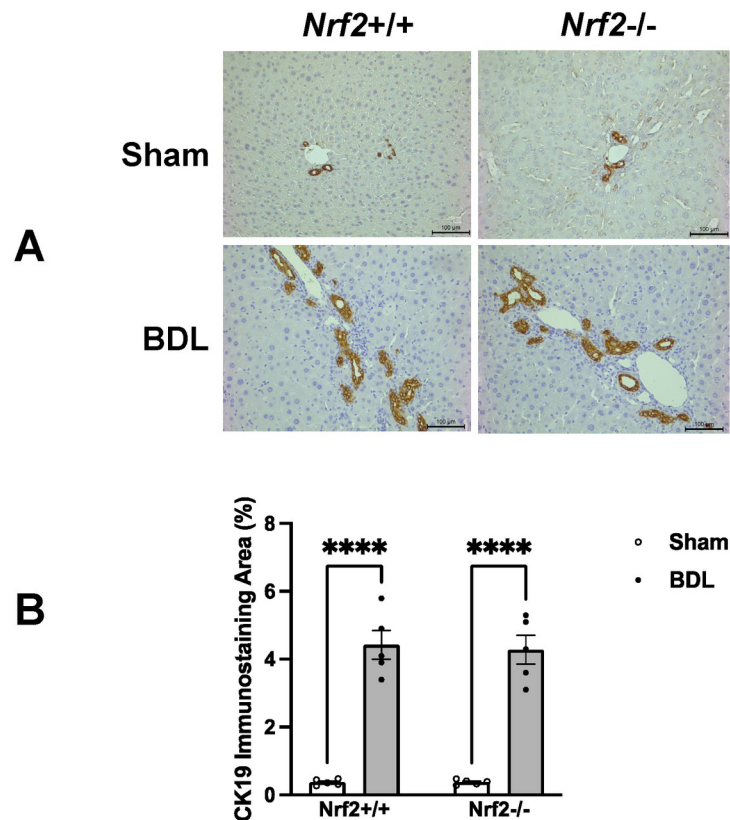


Fig 3. Hepatic distribution of CK19⁺ cells in *Nrf2*^{+/+} and *Nrf2*^{-/-} mice following bile duct ligation (BDL) or sham operation (Sham). Sections were prepared from the livers of mice 40 days after BDL or sham operation and subjected to CK19 immunostaining. (A) Representative sections show CK19⁺ cells stained dark brown within the biliary ducts. (B) The percentages of CK19⁺ areas. Data are presented as mean percentage \pm SEM (n = 5). ****, $P < 0.0001$.

<https://doi.org/10.1371/journal.pone.0269383.g003>

hepatic progenitor marker CD133 and tumor necrosis factor-like weak induced apoptosis receptor (Fn14), as well as epithelial differentiation factor DMBT1. Western blot (Figs 6B and S1) and immunohistochemistry (Fig 7) analyses showed that, as cholestasis progressed to day 15 after BDL, the hepatocytes in the wild-type mice showed very low expression levels of CD133 and Fn14. This observation indicated that hepatocytes underwent slight dedifferentiation. However, during this period, Nrf2 deficiency strengthened the extent of hepatocyte dedifferentiation, as indicated by earlier and stronger induction of CD133 and Fn14 expression. In parallel, after BDL, the hepatocytes induced low DMBT1 expression regardless of Nrf2 expression. Surprisingly, when cholestasis advanced to day 40 post-BDL, the hepatocytes in the wild-type mice not only enhanced Fn14 expression, indicative of increased dedifferentiation, but also drastically upregulated DMBT1 expression. This observation suggested that hepatocytes in the wild-type mice might elevate DMBT1 expression to prevent further dedifferentiation. In contrast, at the same stage of cholestasis, hepatocytes in the Nrf2-null mice retained Fn14 expression but strikingly increased CD133 expression, indicative of more severe dedifferentiation, which was accompanied by the prevention of DMBT1 upregulation. This finding implied that the absence of Nrf2 caused marked hepatocyte dedifferentiation or severe impairment of hepatocyte identity, possibly due to diminished DMBT1 upregulation. Functionally, sham-operated mice produced equivalent amounts of albumin regardless of genotype. However, in response to cholestasis, wild-type hepatocytes persistently increased albumin production, whereas Nrf2-null hepatocytes did oppositely (Figs 6B and S1). By Day 40 following BDL,

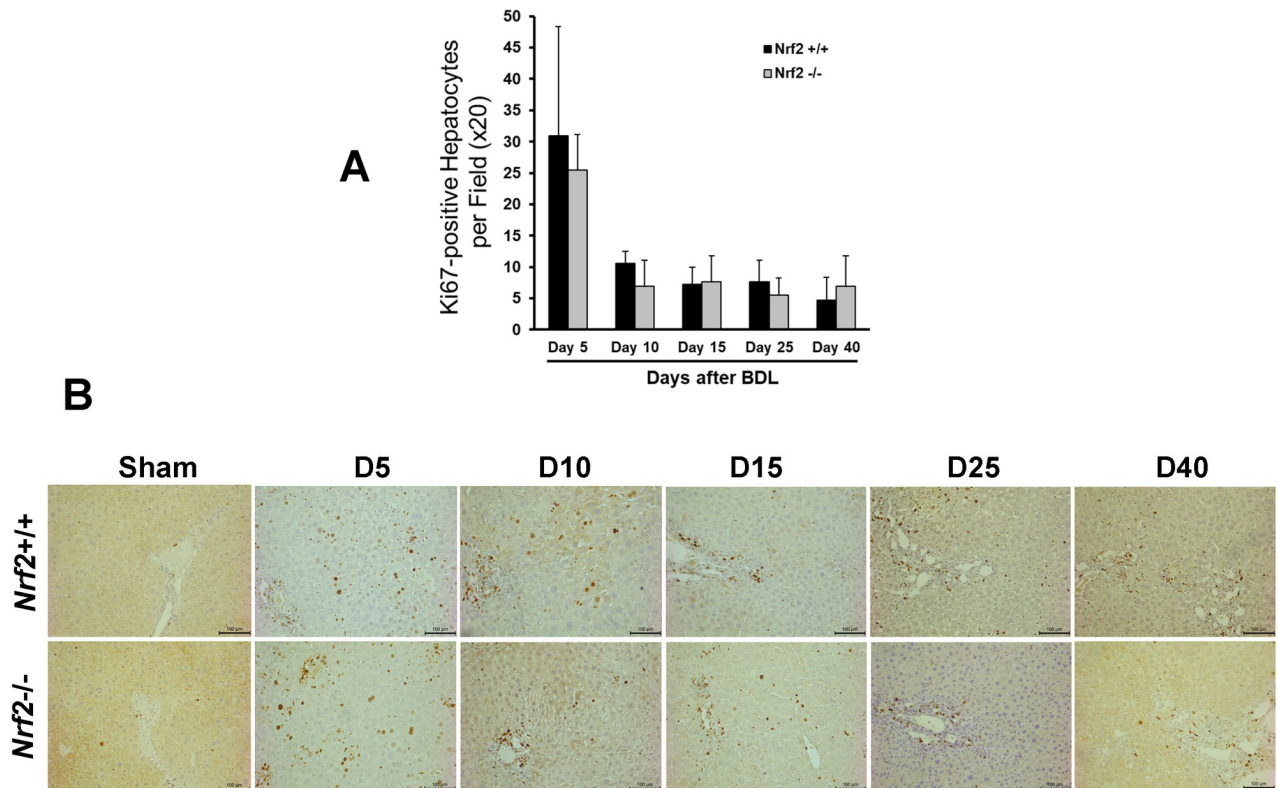


Fig 4. Hepatocyte proliferation induced by bile duct ligation (BDL) in *Nrf2*^{+/+} and *Nrf2*^{-/-} mice. Ki-67 immunostaining was performed using the formalin-fixed and paraffin-embedded liver sections prepared from the livers of mice after BDL or sham operation. (A) Ki67+ hepatocytes were counted at 200x magnification in 5 randomly chosen fields per section. The results are shown as means per field \pm SD (n = 5). (B) Representative liver sections showing Ki67+ cells with the nuclei stained dark brown.

<https://doi.org/10.1371/journal.pone.0269383.g004>

albumin expression levels in *Nrf2*-null mice were only about one fourth of that in wild-type mice. On one hand, this was a functional indication of hepatocyte dedifferentiation owing to the lack of *Nrf2* during cholestasis. On the other hand, the data showed that *Nrf2* deficiency-caused hepatocyte dedifferentiation resulted in adverse consequence in liver function. Collectively, our results demonstrated that *Nrf2* modulated hepatocyte phenotypes possibly via the *Nrf2*/*DMBT1* pathway during cholestasis.

Hepatocytes highly inactivated the yes-associated protein 1 (YAP) and activated the mammalian target of rapamycin (mTOR) signaling to adapt to cholestasis, which is mildly influenced by the lack of *Nrf2* expression

YAP has been shown to regulate hepatocyte differentiation [14, 15]. YAP activation causes hepatocyte dedifferentiation into liver progenitors [15]. We found that the livers after BDL remarkably and persistently increased the expression of phosphorylated (inactivated) YAP and total YAP compared to those of the sham controls in both genotype groups of mice. By day 40 post-BDL, livers of *Nrf2*-null mice showed a significant, but very mild, reduction in the expression of p-YAP compared to those in the wild-type controls (Figs 6B and S1). mTOR signaling is central in regulating cellular metabolism and growth [16] and promotes the dedifferentiation of biliary cells to liver progenitor cells [17]. We observed that the livers in both the wild-type and *Nrf2*-null mice markedly and continuously upregulated the expression of p-mTOR and total mTOR in response to BDL compared to those of the sham controls. When

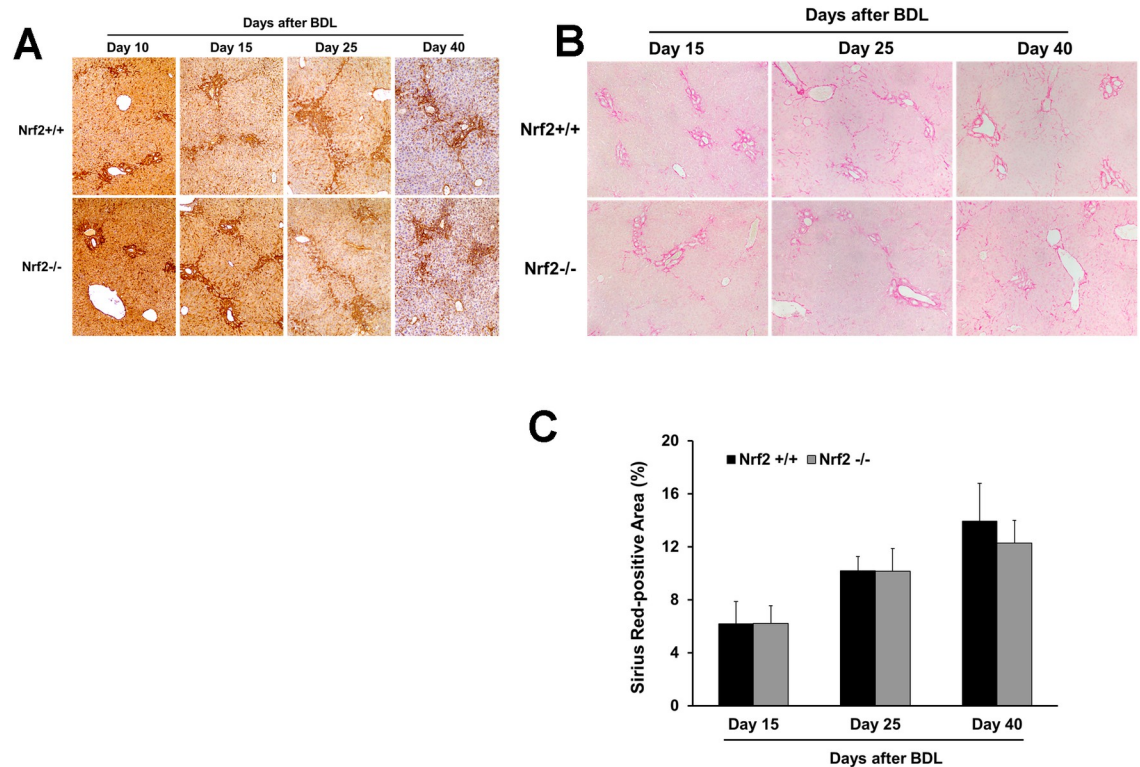


Fig 5. Hepatic fibrotic response to bile duct ligation (BDL) in *Nrf2*^{+/+} and *Nrf2*^{-/-} mice. The liver sections from the livers of mice after BDL underwent laminin immunostaining or Sirius Red staining. (A) Representative liver sections with laminin immunostaining. The septal tissue rich in laminin was stained prominently dark brown. (B) Representative liver sections with Sirius Red staining. (C) Sirius Red staining areas were quantified using Image-Pro Plus software at 200x magnification in 5 randomly chosen fields per section. The results are shown as the means of percentages \pm SD (n = 5).

<https://doi.org/10.1371/journal.pone.0269383.g005>

comparing the two genotype groups of mice, *Nrf2* loss of function led to increased total mTOR expression on days 5 and 15 after BDL (Figs 6B and S1). *Nrf2* is associated with EGFR signaling in the liver [18] and EGFR level is associated with the susceptibility of hepatocytes to oxidative stress [19]. We found that, compared to the sham controls, BDL did not induce significant changes in hepatic p-EGFR levels but progressively reduced the total EGFR expression in both genotype groups of mice (Figs 6B and S1). Taken together, these findings suggested that hepatocytes responded to cholestasis by highly inactivating YAP and activating mTOR signaling and, furthermore, *Nrf2* might not play a major role in mediating these responses.

Discussion

The most striking and novel finding in our study is that, in response to cholestasis, hepatocytes need to activate *Nrf2* to remain in their differentiated state. In this pathological condition, hepatocytes that are deficient in *Nrf2* undergo dedifferentiation. Aleksunes et al. examined the effects of *Nrf2* genetic deletion on hepatic NQO1 expression and activity, liver histology, and liver bile acids within 3 days after BDL in mice. They found that *Nrf2* knock-out prevented the induction of NQO1 expression, reduced accumulation of liver bile acids, and did not alter the extent of total hepatocellular necrosis [11]. Weerachayaphorn et al. analyzed serum alanine aminotransferase, liver histology, expression and deposition of hepatic collagen, and expansion and distribution of CK19+ cells 7 days after BDL in wild-type and *Nrf2*-null mice. They found no significant *Nrf2*-dependent differences in these assessments [10]. Here, we evaluated the liver

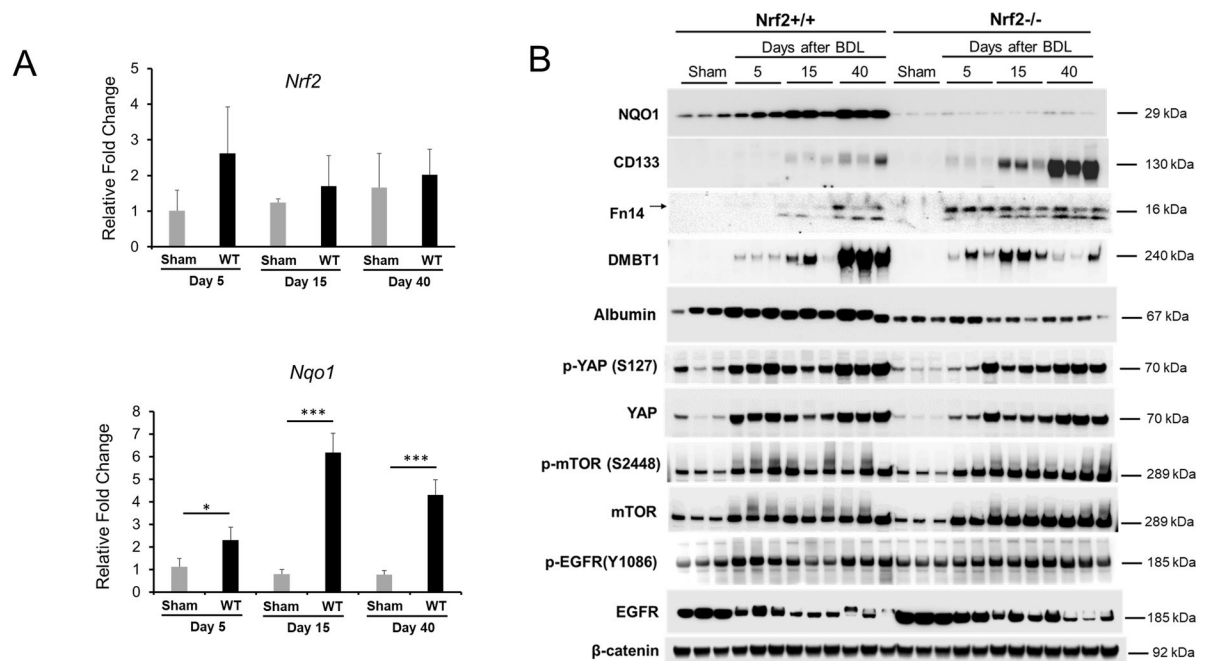


Fig 6. Hepatic expression of a group of genes or proteins in *Nrf2*^{+/+} and *Nrf2*^{-/-} mice after bile duct ligation (BDL). (A) mRNA expression of hepatic *Nrf2* and *Nqo1* was quantified by qRT-PCR. (B) Western blotting was performed with antibodies against the proteins indicated. Liver lysates were prepared from the livers of mice after BDL or sham operation. β-catenon was used as a loading control because it showed the most stable expression over the course of cholestasis relative to regular loading controls screened. Each lane represents a sample from an individual mouse. * $P < 0.05$; ** $P < 0.01$; *** $P < 0.001$.

<https://doi.org/10.1371/journal.pone.0269383.g006>

size, liver injury, biliary ductular reaction, hepatocyte proliferation, and hepatic fibrotic response up to 40 days after BDL and did not observe an overt Nrf2-dependent changes, in line with those two reports. When we extended our study to 40 days after BDL, we observed dedifferentiation of hepatocytes due to Nrf2 deficiency, indicated by a strong CD133⁺/Fn14⁺ phenotype in nearly all of them, which is accompanied by marked reduction in albumin production. CD133 is a cholesterol-binding glycoprotein with an unknown function [20]. Evidence suggests a role for CD133 in the promotion of hepatocellular carcinoma [21]. It is highly expressed in several types of adult stem/progenitor cells, including hematopoietic, neural, and hepatic progenitors. Thus, it is widely used as a marker for stem/progenitor cells in various tissues [22]. Several groups have shown that Fn14 is also expressed in hepatic progenitor cells, and its activation stimulates the expansion of these cells [23–26]. We previously showed that during partial hepatectomy-induced liver regeneration, the absence of Nrf2 caused transient but massive hepatocyte dedifferentiation [27]. Our previous and current findings strongly support a role for Nrf2 in maintaining hepatocyte identity in diseased livers. A recent report showed that, as non-alcoholic steatohepatitis (NASH) progresses, hepatocytes undergo comprehensive reprogramming in their genomics, leading to a loss of their identity and promoting their dysfunction [28]. It is highly likely that, as cholestasis advances, hepatocytes exhibit reprogramming, manifested by impairments in their identity and function, which needs to be further investigated.

The present work also suggests that Nrf2 may not be required for biliary ductular reaction to BDL. Nrf2 has been shown to regulate cholangiocyte differentiation [29]. Taguchi et al. reported that the forced activation of Nrf2 by liver-specific genetic deletion of both its inhibitor Keap1 and phosphatase and tensin homolog led to abnormal expansion of ductal structures containing cholangiocytes, resulting in severe hepatomegaly, which caused animal death

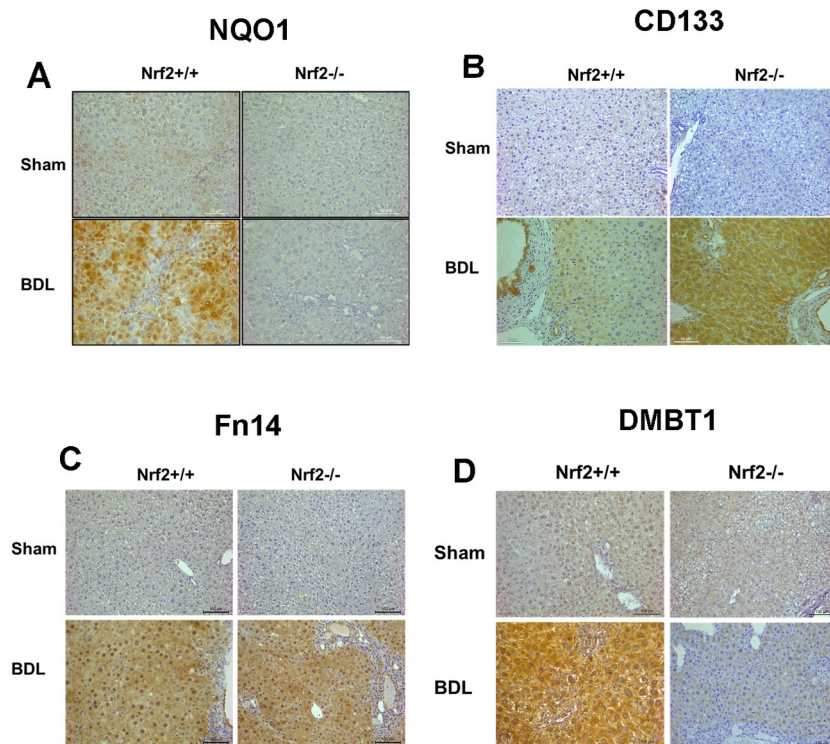


Fig 7. Hepatic distribution of a group of proteins in *Nrf2*^{+/+} and *Nrf2*^{-/-} mice post-bile duct ligation (BDL) or sham operation (Sham). Sections prepared from the livers of mice 40 days after BDL or sham operation were subjected to (A) NQO1, (B) CD133, (C) Fn14, and (D) DMBT1 immunostaining. Representative sections are shown.

<https://doi.org/10.1371/journal.pone.0269383.g007>

within 1 month after birth. This finding demonstrated that Nrf2 activity needs to be tightly controlled to ensure normal cholangiocyte differentiation during development. BDL induces massive ductular reactions with reprogramming or transdifferentiation of hepatocytes to cholangiocytes in order to adapt to cholestasis [30]. We observed progressively increased hepatic Nrf2 activity after BDL, suggesting a role for Nrf2 in hepatic adaptive responses to cholestasis. However, we and others did not observe an obvious effect of the genetic deletion of Nrf2 on BDL-induced biliary ductular reaction. This finding implies that Nrf2 plays distinct roles in cholangiocyte differentiation during different physiological and pathological settings.

The present work identified that the Nrf2/DMBT1 pathway is relevant to the maintenance of hepatocyte phenotypes during cholestasis. Evidence supports the notion that when the liver is chronically injured, a subpopulation of hepatocytes exhibit phenotypic plasticity to promote liver repair [31, 32], whereas most hepatocytes need to stay in the differentiated state to maintain liver function. YAP has been shown to modulate hepatocyte dedifferentiation and differentiation. The activation of YAP expression alone can dedifferentiate hepatocytes to a progenitor phenotype, whereas inactivation of YAP induces differentiation of these cells [15]. However, we found that BDL led to inactivation of hepatic YAP, independent of Nrf2 and irrespective of the change in hepatocyte phenotype. This observation suggested that YAP may not be a gatekeeper of hepatocyte identity in this experimental setting. Remarkably, we found that, in the late stage of cholestasis, hepatocytes abundantly and Nrf2-dependently expressed DMBT1. It has been demonstrated that DMBT1 is essential for epithelial cell differentiation during development [33]. Since the *Dmbt1* gene is deleted in several types of epithelial cancers, it is considered a tumor suppressor. Studies have suggested that DMBT1 may play a dominant

role in forcing the epithelium to maintain its differentiated state [34]. Thus, it is highly likely that hepatocytes activate the Nrf2/DMBT1 pathway to adapt to cholestasis in order to prevent hepatocyte dedifferentiation. In fact, when BDL-induced cholestasis progressed to the late stage, hepatocytes in the wild-type mice displayed a tendency of dedifferentiation, which was reflected by weak CD133 and Fn14 expression. We assume that the concurrent, high magnitude, and Nrf2-mediated elevation of DMBT1 expression prohibits hepatocytes from dedifferentiation, whereas Nrf2 deficiency blocked DMBT1 upregulation, which resulted in a severe impairment in hepatocyte identity. Of note, the correlation of Nrf2 activation with DMBT1 expression was not seen until day 40 after BDL. On this day, Nrf2 activity reached a highest level, indicated by highest expression of its target NQO1, while the expression of DMBT1 was most abundantly induced. This suggests that the level of Nrf2 activity may play a role in upregulating DMBT1. Indeed, Zuker et al. demonstrated that in fibroblasts, Nrf2 is able to directly activate the express of transcription Kruppel-like factor 9 only when Nrf2 activity is high enough to reach a threshold, whereas a low level of Nrf2 activity did not [35]. Therefore, it is likely that Nrf2 activity needs to reach a certain level to induce DMBT1 expression in hepatocytes. We are highly interested in elucidating the role and importance of the Nrf2/DMBT1 pathway in modulating hepatocyte phenotypes during liver injury in our future investigation.

Supporting information

S1 Fig. Densitometry of western blotting of Fig 6B. Data are presented as means \pm SD normalized with the loading controls and relative to the sham controls (day 40 after surgery) (n = 3). * $P < 0.05$; ** $P < 0.01$; *** $P < 0.001$.

(TIF)

S1 Raw images.

(PDF)

Author Contributions

Conceptualization: Jingmei Lin, Huaizhou Jiang, Guoli Dai.

Data curation: Guo-Ying Wang, Veronica Garcia, Joonyong Lee, Jennifer Yanum, Huaizhou Jiang.

Formal analysis: Guo-Ying Wang, Veronica Garcia, Joonyong Lee, Jennifer Yanum.

Funding acquisition: Guoli Dai.

Investigation: Veronica Garcia, Jingmei Lin, Huaizhou Jiang, Guoli Dai.

Methodology: Guo-Ying Wang, Joonyong Lee, Huaizhou Jiang, Guoli Dai.

Project administration: Guoli Dai.

Resources: Guoli Dai.

Supervision: Guoli Dai.

Validation: Guo-Ying Wang, Veronica Garcia, Joonyong Lee, Jennifer Yanum, Huaizhou Jiang.

Visualization: Guo-Ying Wang.

Writing – original draft: Huaizhou Jiang, Guoli Dai.

Writing – review & editing: Guo-Ying Wang, Jingmei Lin, Guoli Dai.

References

1. Chan K, Lu R, Chang JC, Kan YW. NRF2, a member of the NFE2 family of transcription factors, is not essential for murine erythropoiesis, growth, and development. *Proceedings of the National Academy of Sciences of the United States of America*. 1996; 93(24):13943–8. <https://doi.org/10.1073/pnas.93.24.13943> PMID: 8943040.
2. Huang Y, Li W, Su ZY, Kong AT. The complexity of the Nrf2 pathway: beyond the antioxidant response. *J Nutr Biochem*. 2015. <https://doi.org/10.1016/j.jnutbio.2015.08.001> PMID: 26419687
3. Suzuki T, Yamamoto M. Molecular basis of the Keap1-Nrf2 system. *Free Radic Biol Med*. 2015; 88(Pt B):93–100. <https://doi.org/10.1016/j.freeradbiomed.2015.06.006> PMID: 26117331.
4. Dodson M, Redmann M, Rajasekaran NS, Darley-USmar V, Zhang J. KEAP1-NRF2 signalling and autophagy in protection against oxidative and reductive proteotoxicity. *The Biochemical journal*. 2015; 469(3):347–55. <https://doi.org/10.1042/BJ20150568> PMID: 26205490.
5. Tebay LE, Robertson H, Durant ST, Vitale SR, Penning TM, Dinkova-Kostova AT, et al. Mechanisms of activation of the transcription factor Nrf2 by redox stressors, nutrient cues, and energy status and the pathways through which it attenuates degenerative disease. *Free Radic Biol Med*. 2015; 88(Pt B):108–46. <https://doi.org/10.1016/j.freeradbiomed.2015.06.021> PMID: 26122708.
6. Dodson M, de la Vega MR, Cholanians AB, Schmidlin CJ, Chapman E, Zhang DD. Modulating NRF2 in Disease: Timing Is Everything. *Annual review of pharmacology and toxicology*. 2019; 59:555–75. Epub 2018/09/27. <https://doi.org/10.1146/annurev-pharmtox-010818-021856> PMID: 30256716; PubMed Central PMCID: PMC6538038.
7. Parola M, Leonarduzzi G, Robino G, Albano E, Poli G, Dianzani MU. On the role of lipid peroxidation in the pathogenesis of liver damage induced by long-standing cholestasis. *Free Radic Biol Med*. 1996; 20(3):351–9. [https://doi.org/10.1016/0891-5849\(96\)02055-2](https://doi.org/10.1016/0891-5849(96)02055-2) PMID: 8720905.
8. Tsai LY, Lee KT, Liu TZ. Evidence for accelerated generation of hydroxyl radicals in experimental obstructive jaundice of rats. *Free Radic Biol Med*. 1998; 24(5):732–7. [https://doi.org/10.1016/s0891-5849\(97\)00330-4](https://doi.org/10.1016/s0891-5849(97)00330-4) PMID: 9586803.
9. Liu TZ, Lee KT, Chern CL, Cheng JT, Stern A, Tsai LY. Free radical-triggered hepatic injury of experimental obstructive jaundice of rats involves overproduction of proinflammatory cytokines and enhanced activation of nuclear factor kappaB. *Annals of clinical and laboratory science*. 2001; 31(4):383–90. PMID: 11688850.
10. Weerachayaphorn J, Mennone A, Soroka CJ, Harry K, Hagey LR, Kensler TW, et al. Nuclear factor-E2-related factor 2 is a major determinant of bile acid homeostasis in the liver and intestine. *Am J Physiol Gastrointest Liver Physiol*. 2012; 302(9):G925–36. <https://doi.org/10.1152/ajpgi.00263.2011> PMID: 22345550; PubMed Central PMCID: PMC3362073.
11. Aleksunes LM, Slitt AL, Maher JM, Dieter MZ, Knight TR, Goedken M, et al. Nuclear factor-E2-related factor 2 expression in liver is critical for induction of NAD(P)H:quinone oxidoreductase 1 during cholestasis. *Cell Stress Chaperones*. 2006; 11(4):356–63. Epub 2007/02/07. <https://doi.org/10.1379/csc-217.1> PMID: 17278884; PubMed Central PMCID: PMC1759988.
12. Tanaka Y, Aleksunes LM, Cui YJ, Klaassen CD. ANIT-induced intrahepatic cholestasis alters hepatobiliary transporter expression via Nrf2-dependent and independent signaling. *Toxicol Sci*. 2009; 108(2):247–57. <https://doi.org/10.1093/toxsci/kfp020> PMID: 19181614; PubMed Central PMCID: PMC2664692.
13. Okada K, Shoda J, Taguchi K, Maher JM, Ishizaki K, Inoue Y, et al. Nrf2 counteracts cholestatic liver injury via stimulation of hepatic defense systems. *Biochemical and biophysical research communications*. 2009; 389(3):431–6. <https://doi.org/10.1016/j.bbrc.2009.08.156> PMID: 19732748.
14. Lee YA, Noon LA, Akat KM, Ybanez MD, Lee TF, Berres ML, et al. Autophagy is a gatekeeper of hepatic differentiation and carcinogenesis by controlling the degradation of Yap. *Nature communications*. 2018; 9(1):4962. Epub 2018/11/25. <https://doi.org/10.1038/s41467-018-07338-z> PMID: 30470740; PubMed Central PMCID: PMC6251897.
15. Yimlamai D, Christodoulou C, Galli GG, Yanger K, Pepe-Mooney B, Gurung B, et al. Hippo pathway activity influences liver cell fate. *Cell*. 2014; 157(6):1324–38. Epub 2014/06/07. <https://doi.org/10.1016/j.cell.2014.03.060> PMID: 24906150; PubMed Central PMCID: PMC4136468.
16. Kim J, Guan KL. mTOR as a central hub of nutrient signalling and cell growth. *Nat Cell Biol*. 2019; 21(1):63–71. Epub 2019/01/04. <https://doi.org/10.1038/s41556-018-0205-1> PMID: 30602761.
17. He JB, Chen JY, Wei XY, Leng H, Mu HL, Cai PC, et al. Mammalian Target of Rapamycin Complex 1 Signaling Is Required for the Dedifferentiation From Biliary Cell to Bipotential Progenitor Cell in Zebrafish Liver Regeneration. *Hepatology (Baltimore, Md)*. 2019; 70(6):2092–106. <https://doi.org/10.1002/hep.30790> PubMed PMID: WOS:000480462600001. PMID: 31136010

18. He F, Antonucci L, Yamachika S, Zhang Z, Taniguchi K, Umemura A, et al. NRF2 activates growth factor genes and downstream AKT signaling to induce mouse and human hepatomegaly. *J Hepatol*. 2020; 72(6):1182–95. Epub 2020/02/28. <https://doi.org/10.1016/j.jhep.2020.01.023> PMID: 32105670.
19. Kim MJ, Choi WG, Ahn KJ, Chae IG, Yu R, Back SH. Reduced EGFR Level in eIF2alpha Phosphorylation Deficient Hepatocytes Is Responsible for Susceptibility to Oxidative Stress. *Mol Cells*. 2020; 43(3):264–75. Epub 2020/03/10. <https://doi.org/10.14348/molcells.2020.2197> PMID: 32150794; PubMed Central PMCID: PMC7103887.
20. Corbeil D, Karbanova J, Fargeas CA, Jaszai J. Prominin-1 (CD133): Molecular and Cellular Features Across Species. *Advances in experimental medicine and biology*. 2013; 777:3–24. https://doi.org/10.1007/978-1-4614-5894-4_1 PMID: 23161072.
21. Won C, Kim BH, Yi EH, Choi KJ, Kim EK, Jeong JM, et al. Signal transducer and activator of transcription 3-mediated CD133 up-regulation contributes to promotion of hepatocellular carcinoma. *Hepatology (Baltimore, Md)*. 2015; 62(4):1160–73. <https://doi.org/10.1002/hep.27968> PMID: 26154152.
22. Grosse-Gehling P, Fargeas CA, Dittfeld C, Garbe Y, Alison MR, Corbeil D, et al. CD133 as a biomarker for putative cancer stem cells in solid tumours: limitations, problems and challenges. *The Journal of pathology*. 2013; 229(3):355–78. <https://doi.org/10.1002/path.4086> PMID: 22899341.
23. Yovchev MI, Grozdanov PN, Zhou H, Racherla H, Guha C, Dabeva MD. Identification of adult hepatic progenitor cells capable of repopulating injured rat liver. *Hepatology (Baltimore, Md)*. 2008; 47(2):636–47. Epub 2007/11/21. <https://doi.org/10.1002/hep.22047> PMID: 18023068.
24. Tirnitz-Parker JE, Viebahn CS, Jakubowski A, Klopic BR, Olynyk JK, Yeoh GC, et al. Tumor necrosis factor-like weak inducer of apoptosis is a mitogen for liver progenitor cells. *Hepatology (Baltimore, Md)*. 2010; 52(1):291–302. Epub 2010/06/26. <https://doi.org/10.1002/hep.23663> PMID: 20578156.
25. Jakubowski A, Ambrose C, Parr M, Lincecum JM, Wang MZ, Zheng TS, et al. TWEAK induces liver progenitor cell proliferation. *The Journal of clinical investigation*. 2005; 115(9):2330–40. Epub 2005/08/20. <https://doi.org/10.1172/JCI23486> PMID: 16110324; PubMed Central PMCID: PMC1187931.
26. Karaca G, Xie G, Moylan C, Swiderska-Syn M, Guy CD, Kruger L, et al. Role of Fn14 in acute alcoholic steatohepatitis in mice. *Am J Physiol Gastrointest Liver Physiol*. 2015; 308(4):G325–34. Epub 2014/12/20. <https://doi.org/10.1152/ajpgi.00429.2013> PMID: 25524063; PubMed Central PMCID: PMC4329478.
27. Zou Y, Lee J, Nambiar SM, Hu M, Rui W, Bao Q, et al. Nrf2 is involved in maintaining hepatocyte identity during liver regeneration. *PLoS ONE*. 2014; 9(9):e107423. <https://doi.org/10.1371/journal.pone.0107423> PMID: 25222179; PubMed Central PMCID: PMC4164664.
28. Loft A, Alfaro AJ, Schmidt SF, Pedersen FB, Terkelsen MK, Puglia M, et al. Liver-fibrosis-activated transcriptional networks govern hepatocyte reprogramming and intra-hepatic communication. *Cell Metab*. 2021. Epub 2021/07/09. <https://doi.org/10.1016/j.cmet.2021.06.005> PMID: 34237252.
29. Taguchi K, Hirano I, Itoh T, Tanaka M, Miyajima A, Suzuki A, et al. Nrf2 enhances cholangiocyte expansion in Pten-deficient livers. *Molecular and cellular biology*. 2014; 34(5):900–13. <https://doi.org/10.1128/MCB.01384-13> PMID: 24379438; PubMed Central PMCID: PMC4023823.
30. Yanger K, Zong Y, Maggs LR, Shapira SN, Maddipati R, Aiello NM, et al. Robust cellular reprogramming occurs spontaneously during liver regeneration. *Genes Dev*. 2013; 27(7):719–24. <https://doi.org/10.1101/gad.207803.112> PMID: 23520387; PubMed Central PMCID: PMC3639413.
31. Li W, Li L, Hui L. Cell Plasticity in Liver Regeneration. *Trends Cell Biol*. 2020; 30(4):329–38. Epub 2020/03/24. <https://doi.org/10.1016/j.tcb.2020.01.007> PMID: 32200807.
32. Ko S, Russell JO, Molina LM, Monga SP. Liver Progenitors and Adult Cell Plasticity in Hepatic Injury and Repair: Knowns and Unknowns. *Annu Rev Pathol*. 2020; 15:23–50. Epub 2019/08/11. <https://doi.org/10.1146/annurev-pathmechdis-012419-032824> PMID: 31399003; PubMed Central PMCID: PMC7212705.
33. Gao X, Eladari D, Leviel F, Tew BY, Miro-Julia C, Cheema FH, et al. Deletion of hensin/DMBT1 blocks conversion of beta- to alpha-intercalated cells and induces distal renal tubular acidosis. *Proceedings of the National Academy of Sciences of the United States of America*. 2010; 107(50):21872–7. Epub 2010/11/26. <https://doi.org/10.1073/pnas.1010364107> PMID: 21098262; PubMed Central PMCID: PMC3003085.
34. Vijayakumar S, Takito J, Gao X, Schwartz GJ, Al-Awqati Q. Differentiation of columnar epithelia: the hensin pathway. *Journal of cell science*. 2006; 119(Pt 23):4797–801. Epub 2006/11/30. <https://doi.org/10.1242/jcs.03269> PMID: 17130293.
35. Zucker SN, Fink EE, Bagati A, Mannava S, Bianchi-Smiraglia A, Bogner PN, et al. Nrf2 amplifies oxidative stress via induction of Klf9. *Molecular cell*. 2014; 53(6):916–28. Epub 2014/03/13. <https://doi.org/10.1016/j.molcel.2014.01.033> PMID: 24613345; PubMed Central PMCID: PMC4049522.